

Effect of Contact Inhibition Location on confined cellular organization

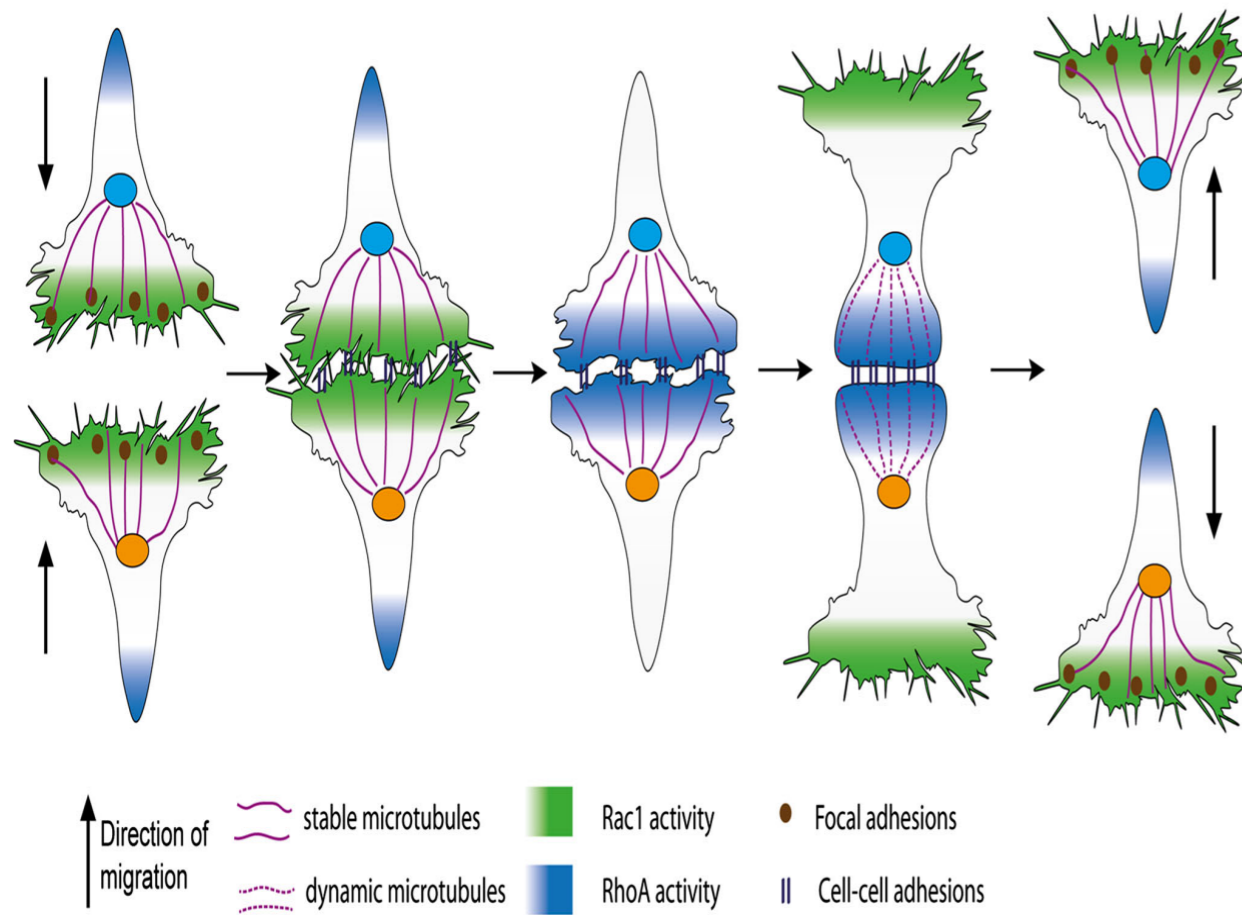
Sudipto Muhuri

Savitribai Phule Pune University

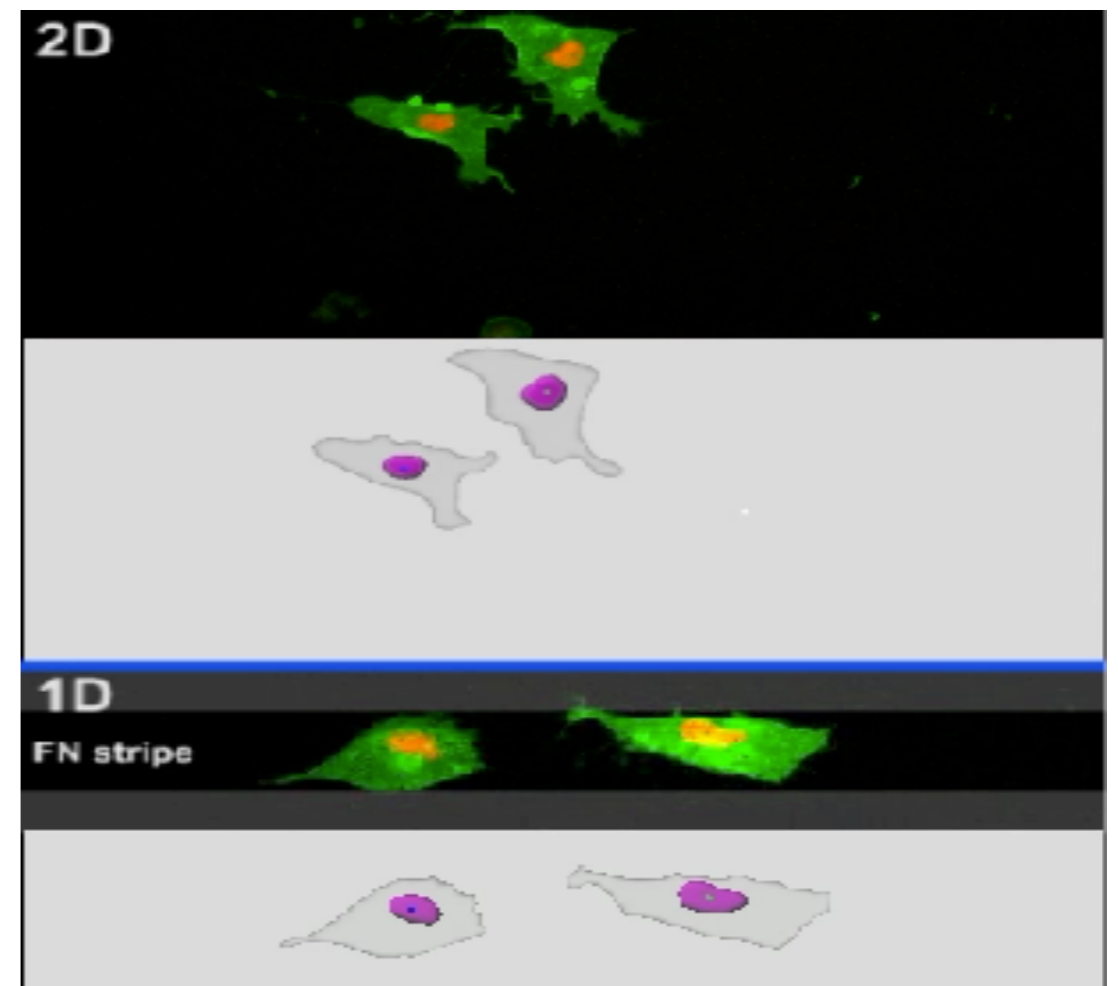


Contact Inhibition Location (CIL)

CIL : Directional reorientation of migrating cells when they come in contact with other cells



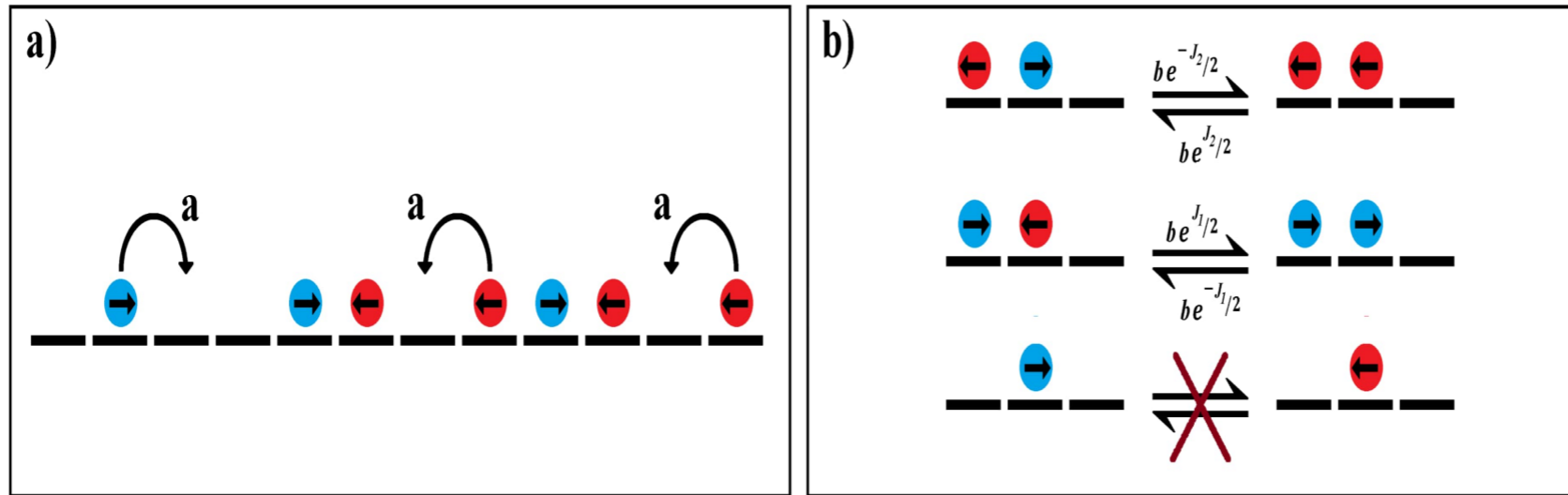
A. Roycroft & R. Mayor, *Cell. Mol. Life Sci.* 73, 1119 (2016)



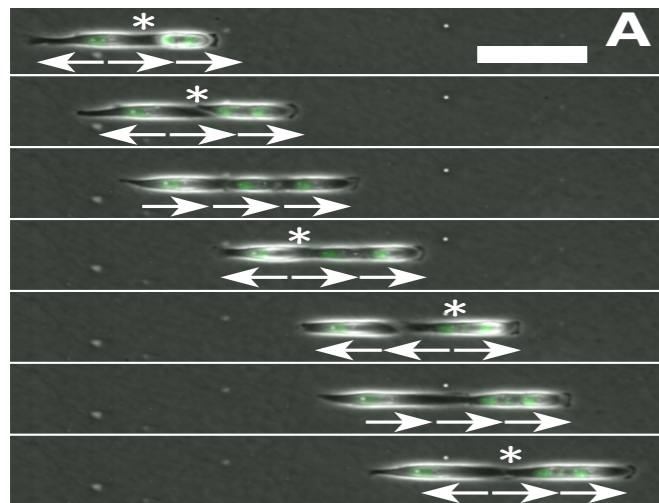
Cell migration on fibronectin coated 1D substrate

(E. Scarpa et.al, *Biol. Open*, 2, 901, 2016)

Model to study effect of CIL on cellular organization in 1D



CIL interaction between particles: $H = \sum_i J_1 \Theta(\sigma_i - \sigma_{i+1}) - J_2 \Theta(\sigma_{i+1} - \sigma_i)$



\rightarrow	\leftarrow	\equiv	$E = +J_1 \quad (J_1 > 0)$
\leftarrow	\rightarrow	\equiv	$E = -J_2 \quad (J_2 > 0)$
\rightarrow	\rightarrow	\equiv	$E = 0$
\leftarrow	\leftarrow	\equiv	$E = 0$

Confluent state: A reduced equilibrium model

- When all the adherent cells fill the fibronectin coated strip, it corresponds to a confluent state
- In confluent state, there are no vacancies in the lattice and there is no translation dynamics
- The dynamics is restricted to switching process between different states of polarization of the particles.

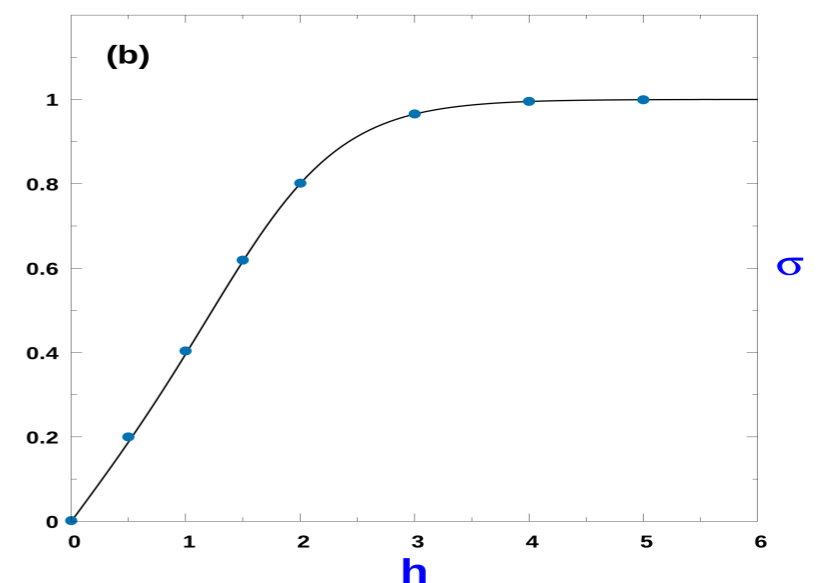
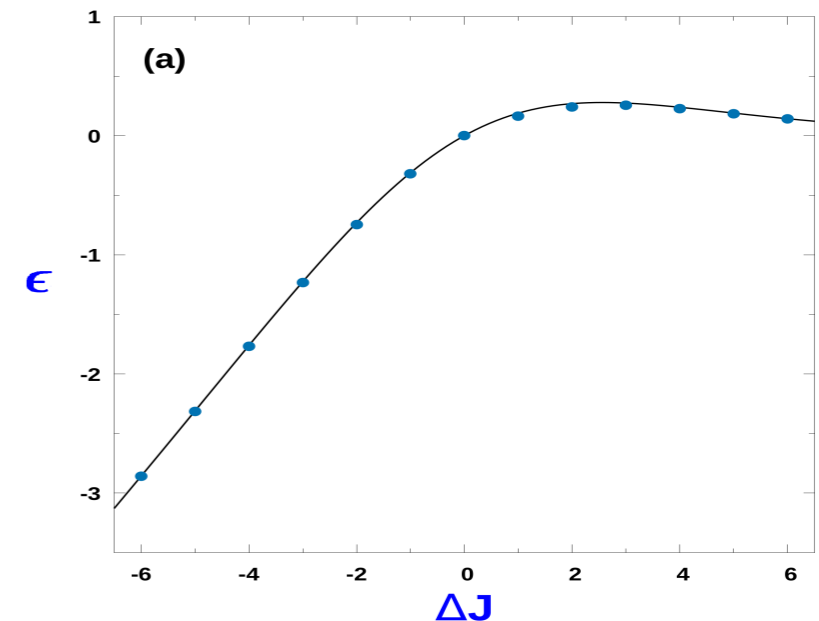
Average Energy: $\langle E \rangle = \frac{N\Delta J}{2} \left[\frac{1}{1 + \exp(\Delta J/2)} \right]$ where $\Delta J = J_1 - J_2$.

Correlation function: $G(r) = \left(\frac{1 - \exp(-\Delta J/2)}{1 + \exp(-\Delta J/2)} \right)^r$

In the limit of $\exp(\Delta J/2) \gg 1$, the correlation length $\xi \rightarrow \frac{1}{2} \exp(\Delta J/2)$

For an external field h which couples to polarization ,

Av. Polarization: $m = \frac{\text{Sinh}(h)}{[\text{Cosh}^2(h) + e^{-\Delta J} - 1]^{1/2}}$



Dynamics & clustering in presence of vacancies

$Q = a / b$: Ratio of hopping and switching rate

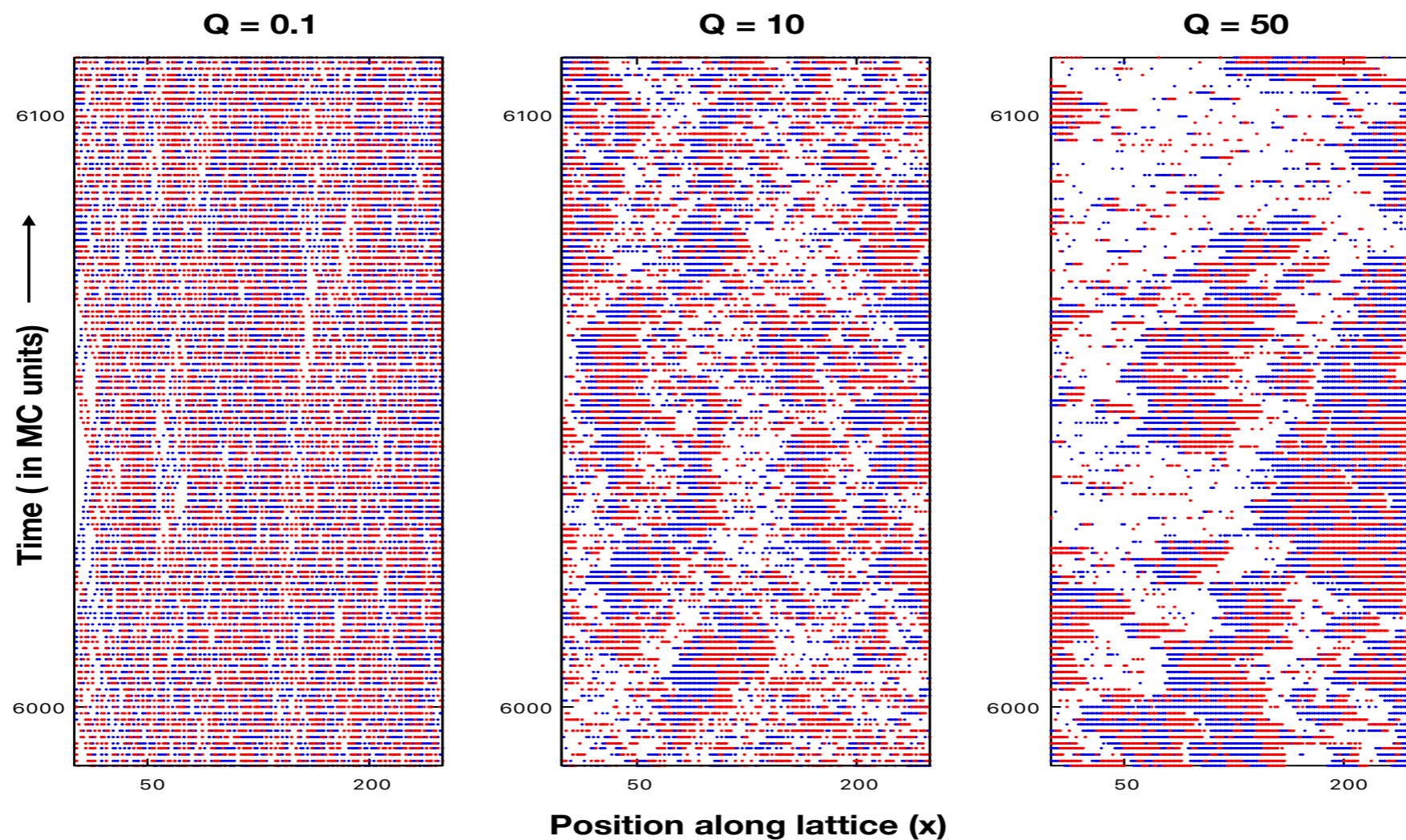


FIG. 3. Spatio-temporal plot: Time snapshots of distribution of right polarized (+)(blue) and left polarized (-)(red) particles on the lattice. Here $Q = 0.1, 10, 50$, $J_1 = 4$, $J_2 = 0$, with $\rho = 0.6$. MC simulations where done with $L = 1000$

Cluster Size distribution

When $Q \ll 1$: $P(m) = \left(\frac{1-\rho}{\rho} \right) e^{-m/\xi}$ (Identical for SEP or TASEP)

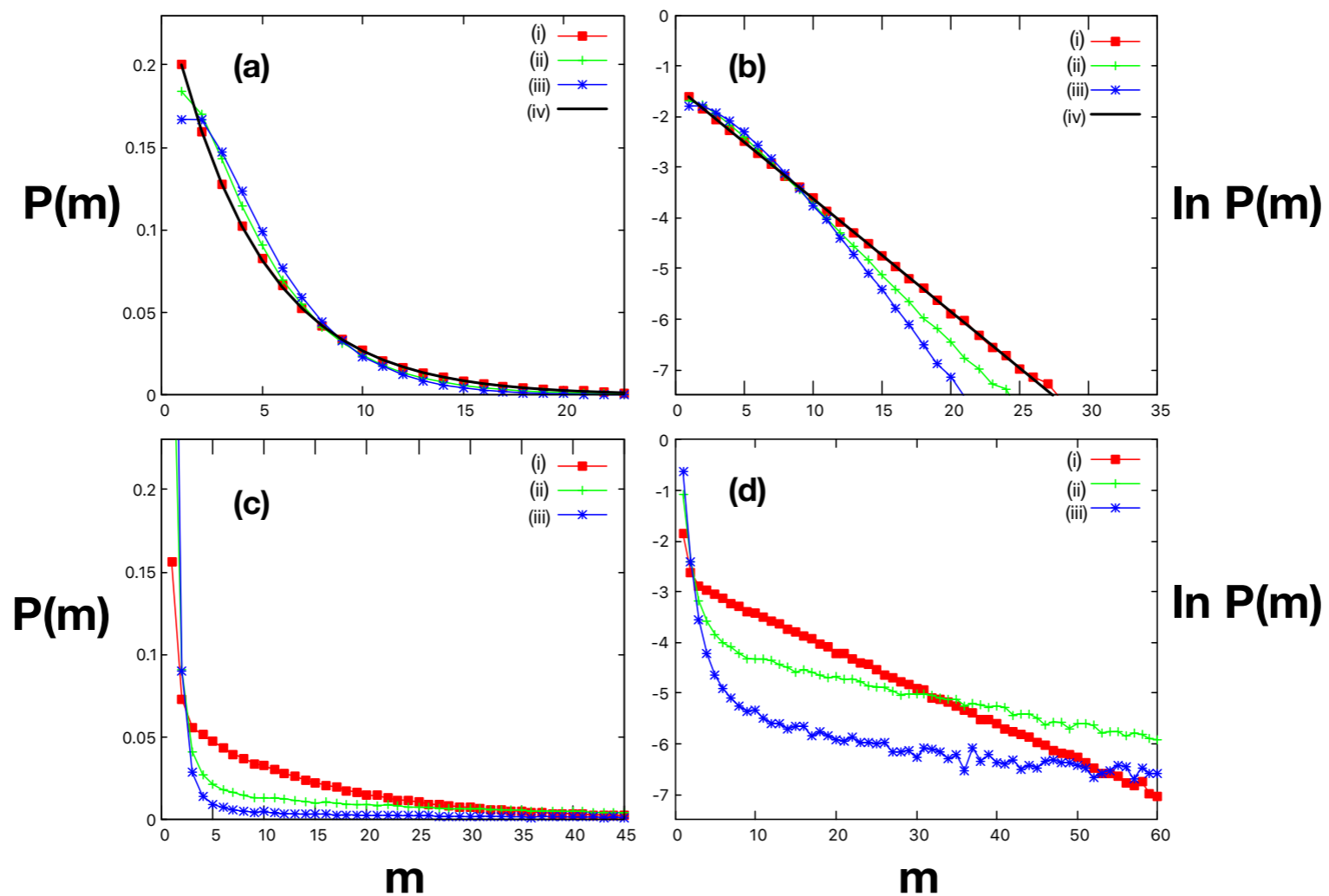
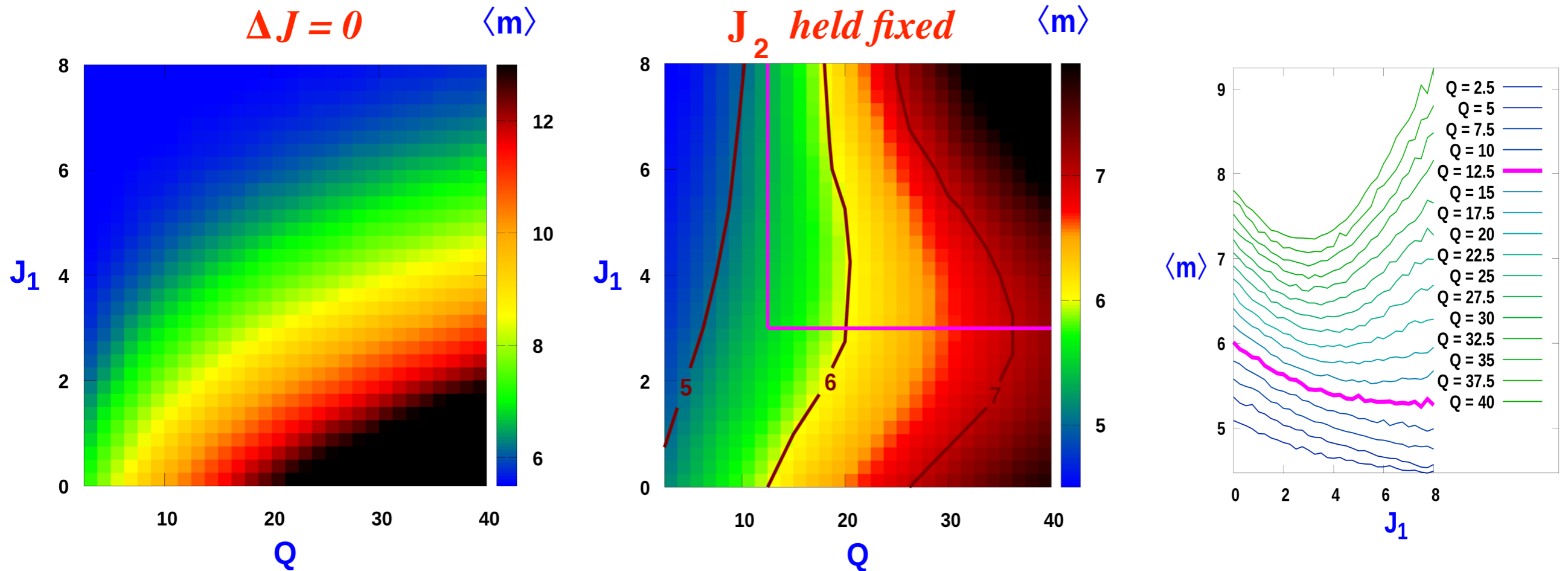


FIG. 4. (a) Probability distribution of cluster size (m) in low Q limit ($Q = 0.1$) for different CIL strength: (i) $J_1 = 0.1$, (ii) $J_1 = 3$, (iii) $J_1 = 7$, (iv) Eq.11 (PDF for TASEP). (b) logplot corresponding to (a). (c) Probability distribution of cluster size (m) in high Q limit ($Q = 30$) for different CIL strength: (i) $J_1 = 0.1$, (ii) $J_1 = 3$, (iii) $J_1 = 7$. (d) logplot corresponding to (c). For all cases, $J_2 = 0$, $\rho = 0.8$, $N = 1000$. MC simulations are performed and averaging is done over 2500 samples.

Contour map of variation of mean cluster size $\langle m \rangle$ with ΔJ and Q



- System exhibits ‘re-entrant’ behavior for cluster size as function of J_1 when $\Delta J \neq 0$

Increasing CIL may increase av. Cluster size !

- For $Q \gg 1$ limit, the average cluster size $\langle m \rangle \sim Q^{1/2}$
- Average cluster size is a monotonically increasing function of Q

Mapping to an equivalent equilibrium process when $Q \gg 1$

- The system comprises of alternate regions of dense Cluster phase (c) & low density gas (g) phase.
- In this limit inter cluster interaction is weak and they evolve independently.
- Problem gets mapped to an equivalent equilibrium process for the sizes of clusters.
- Cluster size distribution is obtained by minimization of Helmholtz Free Energy

Average energy : $\langle E(l) \rangle = \frac{l}{2} \left[\frac{J_1}{1 + e^{J_1/2}} \right]$, when $J_2 = 0$

Configurational Entropy: $S = \ln \left[\frac{C!}{\prod_l G_c(l)!} \right] - \lambda \left(N_c - \sum_l l G_c(l) \right) - \gamma \left(C - \sum_l G_c(l) \right)$

N_c = # of particles in c phase
 G_c = # of clusters of size l
 C = # of clusters

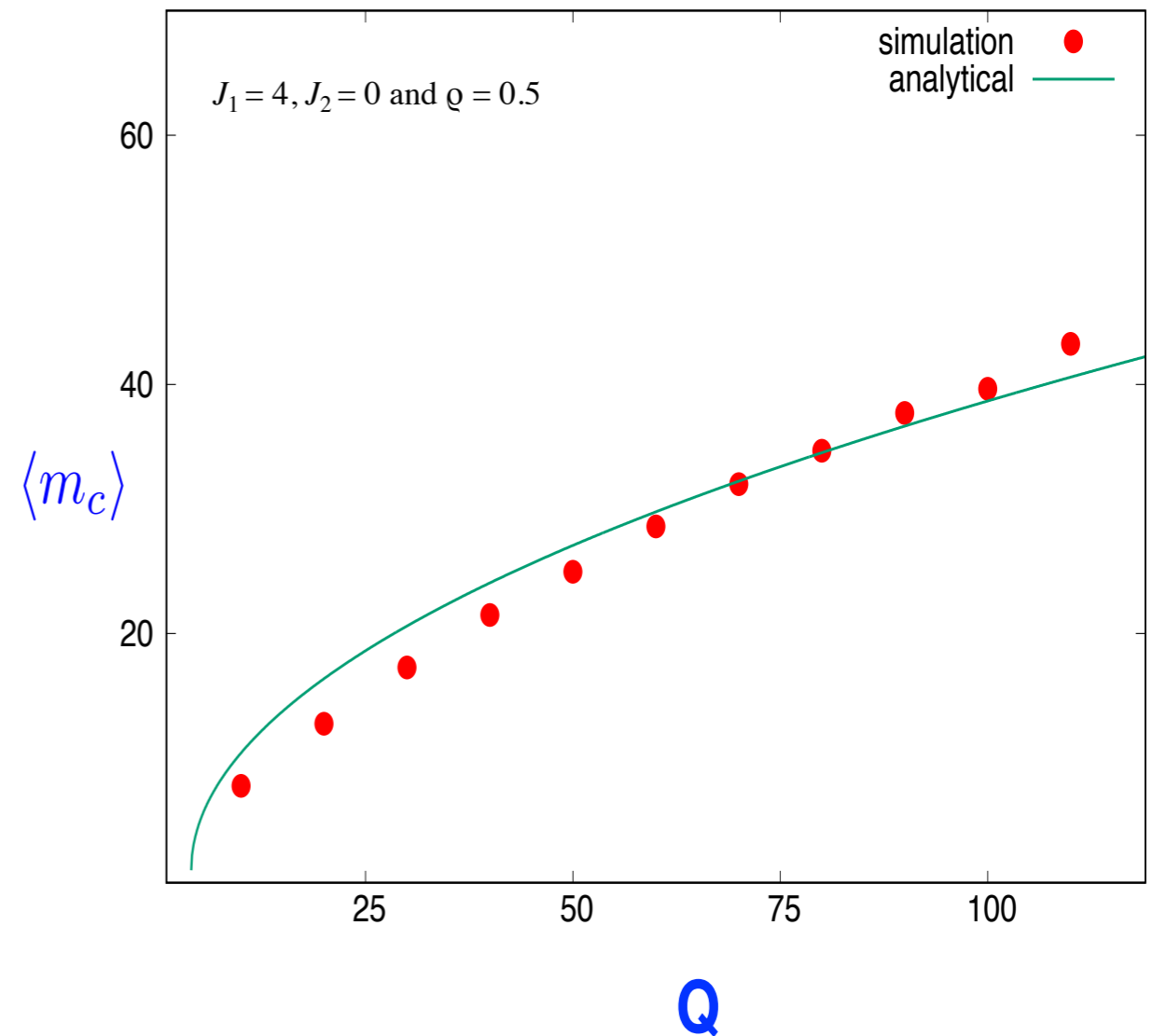
Helmholtz Free energy

$$F = \left[\frac{J_1/2}{1 + e^{J_1/2}} \right] \sum_l l G_c(l) - \ln \left[\frac{C!}{\prod_l G_c(l)!} \right] + \lambda \left(N_c - \sum_l l G_c(l) \right) + \gamma \left(C - \sum_l G_c(l) \right)$$

Approximate expression for average cluster size

$$\langle m_c \rangle = 1 + \sqrt{1 + 2Q \left(\frac{\rho - 2/Q}{1 - \rho} \right) e^{J_1/2}}$$

- Average cluster size $\sim \sqrt{Q}$



Polarization characteristics within Cluster

$$S_F = \frac{1}{m} \sqrt{\left(\sum_{i=1}^m \sigma_i \right)^2}$$

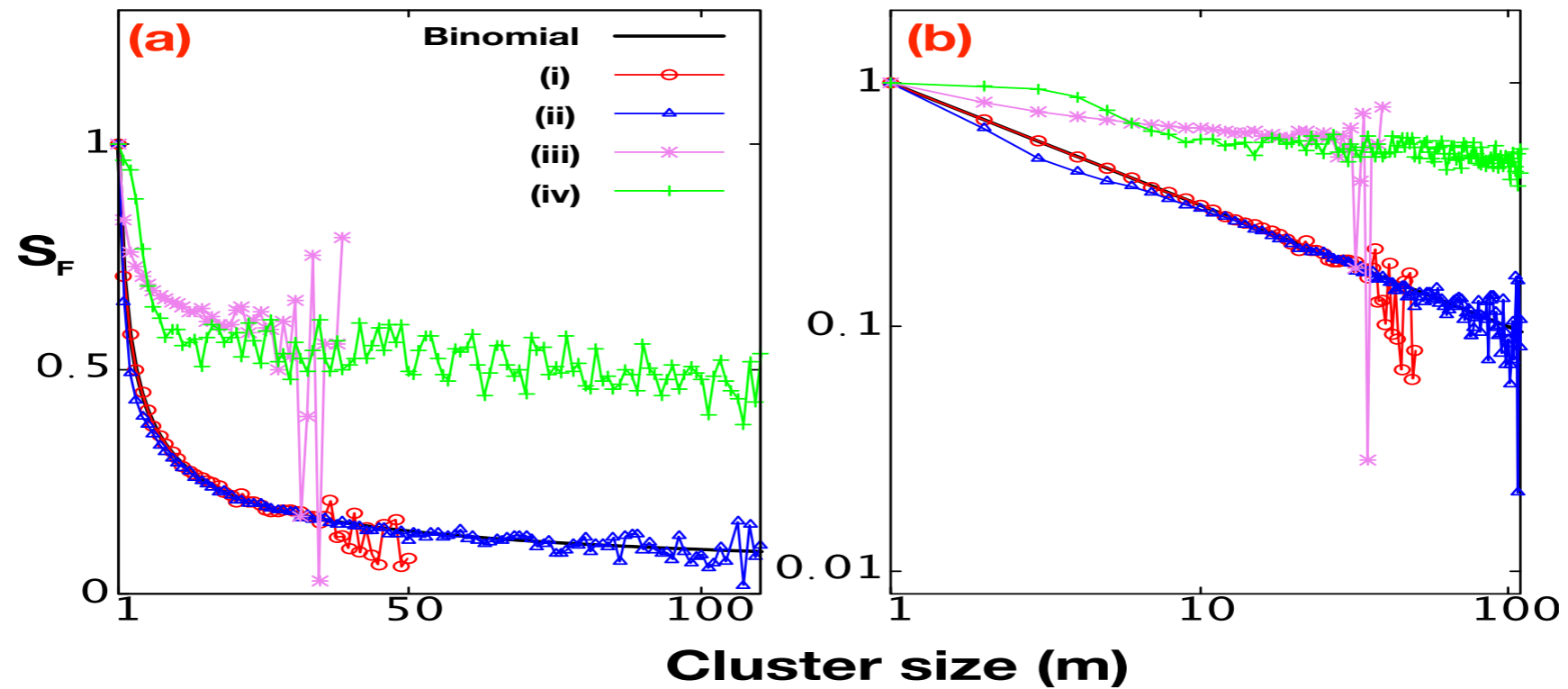


Figure 7. (a) Plot of RMS Fluctuation of Polarization in a cluster of size m (S_F) vs Cluster size (m) : (i) No CIL and low Q ($Q = 0.1$), (ii) No CIL and high Q ($Q = 30$), (iii) $J_1 = 7$ and low Q ($Q = 0.1$), (iv) $J_1 = 7$, high Q ($Q = 30$). The binomial distribution corresponds to solid black line. (b) The corresponding log-log plot for (a). Here $J_2 = 0$, with $\rho = 0.8$. MC simulations were done with $L = 1000$ and averaging was done over 2000 samples.

Effect of external field on cluster characteristics

- The hopping rate of the (\rightarrow) particle becomes $a + h$, while for (\leftarrow) particles, hopping rate is $a - h$

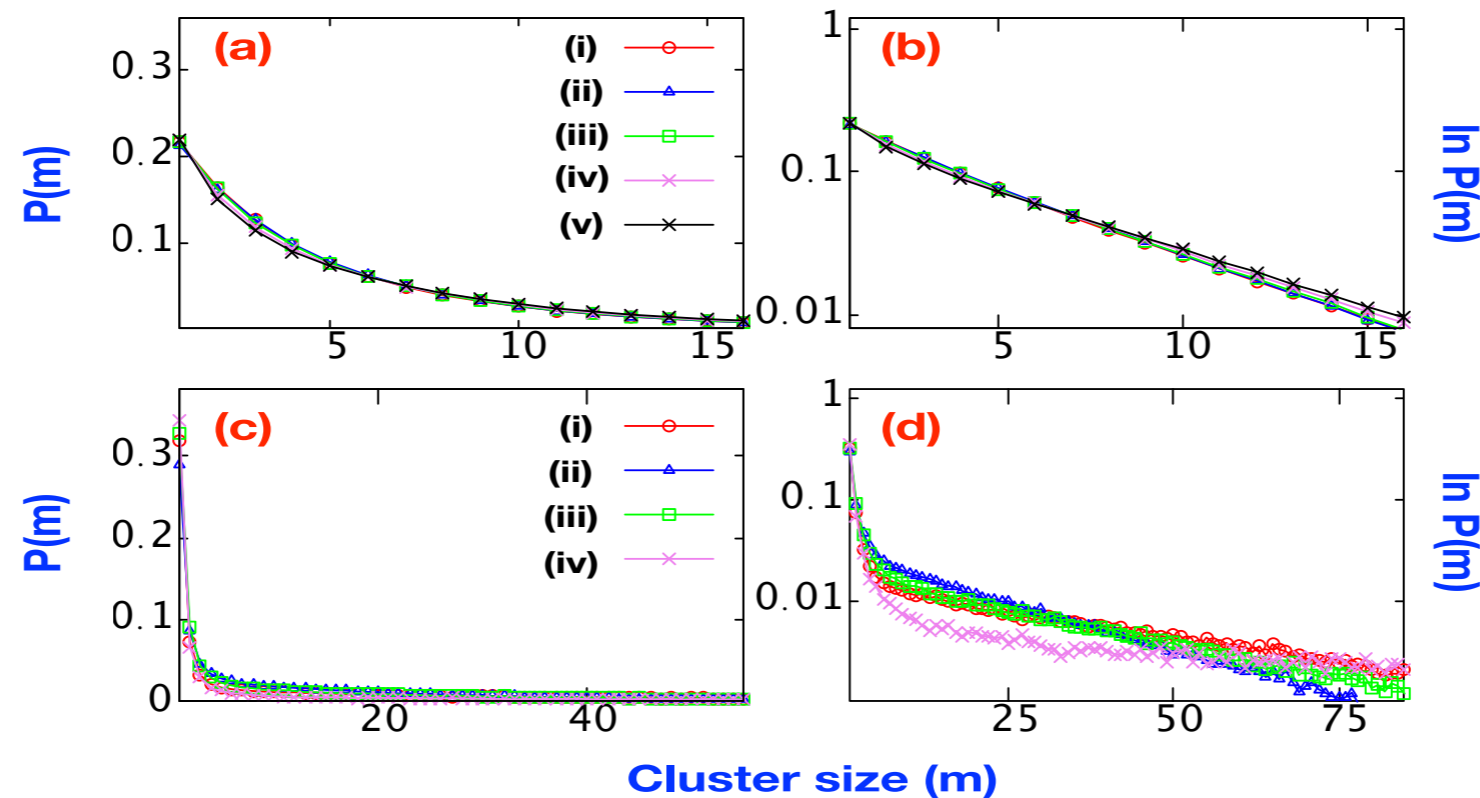


Figure 9. (a) Plot of Cluster size distribution function for low Q ($Q = 1$) with $a = 1$: (i) $h = 0$, (ii) $h = 0.2$, (iii) $h = 0.5$, (iv) $h = 0.9$, (v) $h = 1$. (b) The corresponding logplot for (a). (c) Plot of Cluster size distribution function for high Q ($Q = 50$) with $a = 50$: (i) $h = 0$, (ii) $h = 25$, (iii) $h = 40$, (iv) $h = 50$. (d) The corresponding logplot for (c). Here $J_1 = 3$, $J_2 = 0$ and $\rho = 0.8$. MC simulations were done with $L = 1000$ and averaging was done over 2000 samples.

- Average cluster size varies non-monotonically on increasing h
- As h approaches the hopping rate a , average cluster size sharply increases.

CONCLUSION & OUTLOOK

- For the confluent state (no vacancies), an exactly solvable model discussed
- Average cluster size depends non-monotonically on CIL strength.
- Corresponding contour plot exhibits a 're-entrant' like behavior.
- For $Q \gg 1$ limit, an approximate expression for average cluster size obtained.

- We do not observe any MIPS transition

- How does interplay of CIL with cell-cell adhesion and alignment manifest itself ?
- Generalization to 2D, and comparison with Continuum Hydrodynamic models.

Co-workers



Harshal Potdar
SPPU, pune



Ignacio Pagonabarraga
CECAM, UB

Financial Support : ICTP Associates Program (2022-27)